Bol. Soc. Mat. Mex. (2025) 31:123
https://doi.org/10.1007/s40590-025-00792-y

Sociedad Matemática Mexicana

ORIGINAL PAPER

On a boundary updating method for the scalar Stefan problem

Nikos Barakitis[1] · **Evangelos F. Magirou**[1] · **Paris Vassalos**[1]

Received: 27 December 2024 / Accepted: 22 July 2025 / Published online: 16 September 2025
© The Author(s) 2025

Abstract

In the present work, we propose a general-purpose method for solving the scalar Stefan problem, leveraging a modified version of a well-known boundary updating approach, commonly used in standard existence proofs. Specifically, we consider a Stefan problem with a prescribed positive heat flux at the initial time. Our approach introduces an operator that modifies the phase boundary, such that the fixed points of this operator correspond to solutions of the Stefan problem. The operator is constructed as an integral form of the Stefan condition, and it is shown to be continuous in an appropriate norm. As a result, the existence of a fixed point follows. Moreover, for sufficiently small time horizons, the operator becomes a contraction, enabling a potential method for numerically identifying the boundary. The proposed modification facilitates the numerical solution of a broad class of free boundary problems. We provide a rigorous theoretical justification of the method, along with several computational results that numerically validate its effectiveness. Finally, we present a spectral analysis of the matrix sequence that arises in the discretization of the Stefan problem. Using tools from Generalized Locally Toeplitz (GLT) theory, we characterize the eigenvalue and singular value distributions of the relevant matrix sequence. We identify its spectral symbol and provide a GLT momentary symbol expansion. This analysis enables the design of efficient solvers for the resulting linear systems, and numerical experiments illustrate the method's performance.

Mathematics Subject Classification 35R35 - Free boundary problems · 47H10 - Fixed-point theorems · 47A58 - Operator approximation theory · 65M06 - Finite difference methods for PDEs

✉ Paris Vassalos
pvassal@aueb.gr

Nikos Barakitis
nickbar@aueb.gr

Evangelos F. Magirou
efm@aueb.gr

[1] Athens University of Economics and Business, Patission 76, 10434 Athens, Greece

1 Introduction

The Stefan problem is arguably the most well-known example of a free boundary value problem in the theory of partial differential equations. It concerns the heat equation and, more specifically, the distribution of heat in a phase-changing medium, i.e., within a spatial domain that evolves over time (see e.g., [5, 9, 16]). The phase change—commonly from ice to liquid—occurs at the moving boundary, with the liquid domain advancing into the solid ice. The location of this boundary is unknown a priori and must be determined as part of the solution. The first comprehensive study of this type of problem, focused on the transition between ice and water, was carried out by Joseph Stefan in the late 19th century. This specific formulation is also known as the solidification and melting problem.

Since then, the Stefan problem has been extended and generalized in numerous directions. Applications include the storage of solar energy, modeling of porous media, fresh and saltwater groundwater interaction, penetration of solvents into glassy polymers, and Hele-Shaw flows (see [25] and the references therein). In all these variations, the absence of a fixed boundary, or the partial indeterminacy of the boundary, necessitates the imposition of new conditions on the unknown functions. These conditions are derived from the principle of energy conservation across the moving boundary. While analytical solutions have been studied and found for a limited class of special cases [19], most free boundary problems remain analytically intractable. Consequently, numerical solutions are not only desirable but, in many practically relevant cases, indispensable.

For one-dimensional phase-change (Stefan) problems, a standard scenario involves an infinite rod of ice at zero temperature. The phase change begins with the introduction of a thin liquid layer at one end of the rod. A key challenge is how to initialize the computation of the boundary evolution. A common strategy is to derive an analytical starting solution for the system and use this as an input to the numerical scheme after a small, arbitrarily chosen time interval [20]. In this approach, the numerical scheme proceeds from the analytically determined initial temperature distribution near the origin. A drawback of this approach is that it introduces an artificial singularity into the governing equations. This issue, however, this criticism is addressed in [20], where it is demonstrated that the approach remains valid for several well-known cases in the literature. Nevertheless, the broader question of how to compute the analytic solution for general free boundary problems remains open.

In the current study, we focus on a method for solving such problems without relying on an external or precomputed initial solution. Our approach draws inspiration from the boundary updating method used in existence proofs for Neumann problems, as in [1]. Specifically, we introduce an operator that modifies the position of the phase boundary. The fixed points of this operator correspond to the solutions of the Stefan problem. We show that this operator is continuous in an appropriate norm, thereby guaranteeing the existence of a fixed point. Moreover, we demonstrate that for sufficiently small time horizons, the operator becomes a contraction, thereby offering a potential computational method for locating the boundary. Unlike methods that handle Dirichlet boundary conditions, which typically require different techniques for

existence proofs (see [6, 10]), our approach is applicable to the Stefan problem with Neumann boundary conditions.

We introduce a key modification to this method that improves the operator's contraction properties. Specifically, if the original operator is bounded, our modified technique produces a contraction. This is achieved using a "reversal property" argument: if one function dominates another, then their respective transforms exhibit a reversed dominance relationship. Consequently, by starting with a function that is initially dominated by the fixed point, repeated applications of the operator lead to oscillations around the fixed point. Building on ideas used in the scalar case, we show that it is possible to reduce the amplitude of these oscillations by introducing a weighted average of the identity operator and the original operator, and thus obtaining an algorithm with geometric convergence to the fixed point of Neumann-type problems. The algorithm was applied successfully to several problems in the literature as well as to novel ones.

To illustrate the effectiveness of our method, we apply it to standard cases from the literature, including those found in [1, 20]. Our approach successfully recovers the analytic solution in these standard cases without requiring any additional analysis near the origin to initialize the computation. We further demonstrate the method's ability to solve new and more challenging free boundary problems, including those with both Dirichlet and Neumann boundary conditions. We also extend our approach to handle Stefan conditions for inhomogeneous ice, showing that the method remains robust under these more general conditions.

Another contribution of this study is the spectral analysis of the matrix sequence that appears on the left side of the discretized system. This matrix sequence, denoted $\{L_N\}_N$, arises naturally from the space–time discretization of the system. Using tools from Generalized Locally Toeplitz (GLT) theory (see [11, 12]), we identify its eigenvalue and singular value distributions. The concept of a GLT matrix-sequence provides a natural framework for understanding the spectral properties of discretized linear system. We prove that $\{L_N\}_N$ belongs to the unilevel scalar $*$-algebra of GLT matrix-sequences, and we compute its spectral symbol. Moreover, we derive the GLT momentary symbol expansion for the matrix sequence, which reveals crucial insights into its asymptotic behavior as N tends to infinity. Such analysis is essential for designing fast and efficient solvers for the resulting linear systems.

The structure of the paper is as follows: Section 2 introduces the Stefan problem, focusing on boundary condition variations and homogeneity, as well as relevant results from the literature, with particular attention paid to the operators used in existence proofs in [1]. Section 3 presents the main iterative methods introduced in this work and provides a rigorous justification for their validity. In Sect. 4, we discuss the numerical schemes used to implement the proposed methods while in Sect. 5 we analyze and describe the asymptotic distribution of the eigenvalues/eigenvectors of the coefficient matrix of the previous section by GLT theory methods. Numerical results are given in Sect. 6 while Sect. 7 offers concluding remarks and outlines directions for future research.

2 Statement of the free boundary problem

We follow [1, 20] in formulating the one dimensional Stefan problem, where space and time parameters are x and t respectively. Consider the melting of ice, initially occupying the half line $x \geq 0$ as an insulated rod of infinitesimal thickness which is then heated at $x = 0$. The liquid region at time t is from zero to $s(t)$ and we denote it by $Q_s = \{(x,t)|0 < x < s(t),\ t > 0\}$. We are interested in the temperature distribution $U(x,t)$ in the liquid region Q_s, and the solid–liquid interface or boundary $s(t)$, whose location is not known and must be determined so that it satisfies a condition involving the latent heat of ice melting and heat diffusion. In the liquid phase Q_s, the temperature $U(x,t)$ satisfies the heat equation

$$\frac{\partial U(x,t)}{\partial t} = \frac{\partial^2 U(x,t)}{\partial x^2}, \qquad 0 < x < s(t),\ t > 0,$$

while in the solid phase $Q_s^c = \{(x,t)|x \geq s(t)\}$, we assume that the temperature is zero everywhere. One can consider the case where there exists initially a liquid phase interval at zero temperature, in which case the problem simplifies; we will assume no such interval. We thus have the conditions

$$s(0) = 0, \tag{1}$$
$$U(0,0) = 0, \tag{2}$$
$$U(s(t),t) = 0. \tag{3}$$

On the liquid–solid boundary, the heat of melting must equal the heat transfer due to the temperature gradient. Thus, if $L = L(x)$ is the latent heat per unit volume, $k = k(x)$ the diffusivity coefficient of the liquid at position x, then $-kU_x(s(t),t)\delta t = L\delta s$; setting $\beta = L/k$, we obtain the Stefan condition

$$\beta(s(t))\frac{ds}{dt} = -\frac{\partial U(s(t),t)}{\partial x}.$$

In case L depends on the position x, a situation that might occur if there are impurities in the solid phase, there is a space dependence $\beta = \beta(x)$. We assume that there are no changes in the diffusivity coefficient k. We will mostly work with a constant β, but our numerical methods work also for $\beta = \beta(x)$.

As in the literature, we consider a two modes of heating, a Dirichlet and a Neumann form and we examine two types of conditions at $x = 0,\ t > 0$

$$U(0,t) = g(t) \geq 0, \qquad \text{Dirichlet boundary} \tag{4}$$
$$-\frac{\partial U(0,t)}{\partial x} = h(t) \geq 0. \qquad \text{Neumann boundary} \tag{5}$$

As customary, we assume g to be nonnegative and h to be positive.

Let $Q_{s,T} = \{(x,t)|0 < x < s(t), 0 < t < T\}$ and $\overline{Q_{s,T}}$ be the closure of $Q_{s,T}$. A solution of the problem consisting of (2),(1)-(3),(2), and either (4) or (5) in the horizon

from zero to T i.e., $Q_{s,T}$ is a pair (U, s) with $s \in C^1((0,T]) \cap C([0,T])$, $s(0) = 0$, $s \geq 0$, $0 \leq t \leq T$, $U \in C(\overline{Q_{s,T}}) \cup C^{2,1}(\overline{Q_{s,T}})$, $U_x \in C(\overline{Q_{s,T}} - \{t = 0\})$. For constant β, there are standard existence and uniqueness theorems for both the Dirichlet and the Neumann condition as long as the heat flux h is positive and the temperature is nonnegative at the origin [1, 6, 7, 10], but the proof of the Neumann case is more relevant to our work.

In the existence proofs, the following construction, transformation proves useful [5]: One considers a function s serving as a candidate for the interface (and hence $s(0) = 0$) and then solves a heat equation problem without the Stefan condition and s as the interface. Namely one considers the solution $U^s(x,t)$ of (2),(1)-(3) and either (4) or (5) in the domain $Q_{s,T}$. We will refer to the problem of finding a solution for given s and a Dirichlet condition (4) as the *Fixed Boundary Dirichlet problem*. Finding a solution $U^s(x.t)$ for s and a Neumann condition (5) will be called the *Fixed Boundary Neumann problem.*

2.1 Boundary transformation for a homogeneous solid

Given a boundary s, consider its transformation by:

$$\mathcal{R}(s)(t) = -\int_0^t U_x^s(s(z), z)/\beta(s(z))\mathrm{d}z \qquad 0 \leq t \leq T.$$

For a uniform solid phase $\beta(x) = \beta$ and with no loss of generality, we assume that $\beta = 1$, and thus the $\mathcal{R}$ transform simplifies to

$$\mathcal{R}(s)(t) = -\int_0^t U_x^s(s(z), z)\mathrm{d}z \qquad 0 \leq t \leq T.$$

It is easily verified that a fixed point s^* of (6) is a solution to the Stefan problem. Our results will be for the homogeneous case, but the proposed numerical methods seem to work even for the inhomogeneous one. We will briefly examine this last case in the next subsection.

Returning to the homogeneous case, using Green's theorem for the identically zero function $U_{xx} - U_t$ on $Q_{s,T}$, we obtain

$$\mathcal{R}(s)(t) = -\int_0^t U_x^s(0, z)\mathrm{d}z - \int_0^{s(t)} U^s(x,t)\mathrm{d}x \qquad 0 \leq t \leq T.$$

For Neumann type problems, this becomes

$$\mathcal{R}(s)(t) = \int_0^t h(z)\mathrm{d}z - \int_0^{s(t)} U^s(x,t)\mathrm{d}x.$$

Using this expression, it can then be shown that $\mathcal{R}$ is continuous in the appropriate norm; by Schauder's theorem (see e.g., [22]), it has a fixed point which is the required solution. Moreover, in [1], it is shown that it is a contraction for a small enough horizon

T, leading thus to a constructive existence proof. This argument is not applicable for the Dirichlet problem (4) since(2.1) does not lead to (6) which is crucial for proving continuity of $\mathcal{R}$. A different approach is used to show existence in [10] or [6] and [7]. However, we will show that the modified operator $\mathcal{R}$ as it is formulated in (2.1), possesses additional properties that can serve as a basis for a general purpose iterative algorithm.

3 An iterative algorithm for free boundary problems

3.1 Fixed point algorithms for the homogeneous case

For the homogeneous solid, a useful property of $\mathcal{R}$ is stated as an exercise in [1]. We state and prove it next.

Lemma 3.1 (Reversal Lemma) *Consider the Fixed Boundary Neumann Problem as defined in the previous section (Namely the solution U^s of (2),(1)-(3) and the Neumann condition (5)) and assume that it has a solution for any smooth s starting at the origin. If s_1, s_2 are boundary functions such that $s_1(t) \leq s_2(t), \ t \in [0, T]$ then $\mathcal{R}(s_1)(t) \geq \mathcal{R}(s_2)(t)$.*

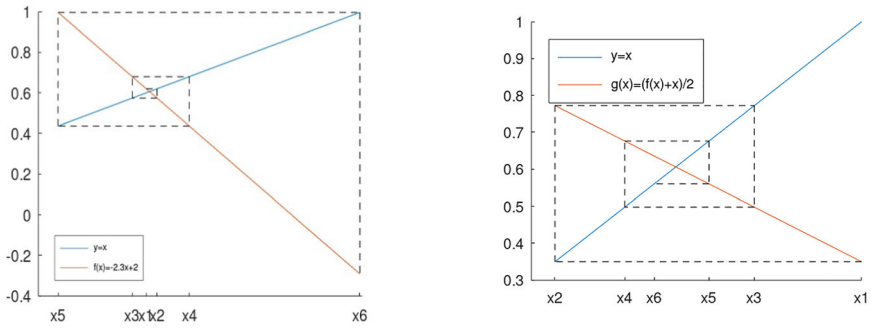
Proof We assumed the existence of $U^s, \ s = s_1, s_2$. Assuming that $h > 0$ we will first show that U^s is everywhere nonnegative. If not, since U^s is zero on the boundary s and it attains its extremes on the parabolic boundary, the minimum must be at some $(x, t) = (0, t^*)$. If the minimum is negative, then $U^s(0, t^*) < 0$. But since $U^s_x(0, t^*) = -h(t^*) < 0$, the minimum cannot be at $(0, t^*)$ and by this contradiction, it follows that U^s is nonnegative on $Q_{s,T}$.

Consider now the solutions of the above problem in the boundaries $s_1, s_2 U^{s_1,\epsilon}$ and U^{s_2} respectively with Neumann conditions $-U^{s_1,\epsilon}_x(0, t) = h(t) + \epsilon$,$-U^{s_2}_x(0, t) = h(t)$. Also consider their difference $\Delta^\epsilon(t) = U^{s_2}(t) - U^{s_1,\epsilon}(t)$. On s^1, $\Delta^\epsilon \geq 0$ and if its minimum is negative, it occurs on a zero value of x. But this is impossible since $\Delta^\epsilon_x(0, t) = -\epsilon < 0$ and thus $\Delta^\epsilon \geq 0$. As $\epsilon \to 0$ and assuming continuity with ϵ, we obtain $\lim_{\epsilon \leftarrow 0} \Delta^\epsilon = U^{s_2} - U^{s_1} \geq 0$ everywhere. Then using (6), we have

$$\begin{aligned} \mathcal{R}(s_1)(t) - \mathcal{R}(s_2)(t) &= \int_0^{s_2(t)} U^{s_2}(x, t)\mathrm{d}x - \int_0^{s_1(t)} U^{s_1}(x, t)\mathrm{d}x \\ &= \int_0^{s_1(t)} [U^{s_2}(x, t) - U^{s_1}(x, t)]\mathrm{d}x + \int_{s_1(t)}^{s_2(t)} U^{s_2}(x, t)\mathrm{d}x. \quad (6) \end{aligned}$$

Since both terms are nonnegative, we have $\mathcal{R}(s_1) \geq \mathcal{R}(s_2)$. □

This *Reversal Property* 3.1 is reminiscent of a modification in one-dimensional fixed point algorithms (see Fig. 1), suitable for functions f with large, negative slopes where we use instead of f a combination of f and the identity. The iteration $x_{n+1} = f(x_n)$ is diverging, but the iteration $x_{n+1} = g(x_n)$ with $g(x) = (f(x) + x)/2$ has a better chance of converging, being of smaller absolute slope.



(a) The standard Fixed-Point iteration diverges. (b) The modified iteration converges.

Fig. 1 Impact of function slope on Fixed-Point convergence

Using the Reversal Property, we can construct a fixed point iteration that converges theoretically but without any speed guarantee. We will write $s_1 \leq s_2$ if $s_1(t) \leq s_2(t) \quad t \in [0, T]$ and $s_1(t_1) > s_2(t_1)$ for some t_1 and also $s_1 = s_2$ if the equality holds for all t. Consider the fixed point s^* and construct an initial boundary $s_0 \leq s^*$ as follows: In the Neumann case, s^* is bounded by Mt with $M = \max_{0\leq\tau\leq t}[-h(\tau)]$, and thus by the Reversal Property $\mathcal{R}(Mt) \leq s^*$. Then $s_1 = \mathcal{R}(s_0) \geq s^*$ and $\mathcal{R}(s_1) \leq s^*$ as well as $s_0 \leq s^*$; however, we do know the relation between $\mathcal{R}(s_1)$ and s_0. Now if $\mathcal{R}(s_1) \geq s_0$ or $\mathcal{R}(s_1) \neq s_0$, we can set $s_2 = max[\mathcal{R}(s_1), s_0]$ and thus, $s_0 \leq s_2 \leq s^*$. Proceeding this way, we generate a sequence

$$s_0 \leq s_2 \leq \ldots \leq s_{2k} \leq \ldots \leq s^* \leq \ldots \leq s_{2k+1} \leq \ldots \leq s_3 \leq s_1,$$

This sequence will converge to s^* provided for no k, we have $\mathcal{R}(s_k) = s_{k-1}$, in which case the iteration oscillates between s_k and s_{k-1}. Furthermore, if in the second iteration, we had $\mathcal{R}(s_1) \leq s_0$, the iterates s_n will diverge. To remedy both problems, consider the family of candidate boundaries

$$\mathcal{P}^\alpha(s)(t) = \alpha\mathcal{R}(s)(t) + (1-\alpha)s(t), \qquad \alpha \in [0, 1]. \tag{7}$$

Clearly, $\mathcal{P}^0(s_1) = s_1 \geq s^* \geq s_0, \mathcal{P}^1(s_1) \leq s_0$. Thus, for some $\alpha' \in (0, 1)$, we have $s_0 \leq \mathcal{P}^{\alpha'}(s_1) \leq s^*$ and $\mathcal{P}^{\alpha'}(s_1) \neq s_0$. Therefore, the iteration can proceed by setting $s_2 = \mathcal{P}^{\alpha'}(s_1)$. A similar fix is possible in the oscillatory case $\mathcal{R}(s_k) = s_{k-1}$ in which case we set $s_k = \mathcal{P}^{\alpha'}(s_{k-1})$ for an α' close to 1. Of course, to apply this in practice, we must show how to select appropriate α's.

This problem with the fixed point iteration can be remedied in the Neumann case if we exploit the boundedness of $\mathcal{R}$ ([1]) to obtain operators $\mathcal{P}^\alpha(s)$ that are contractions. We will do so in the next two Propositions. The following proposition demonstrates that $\mathcal{P}^{1/2}$ exhibits superior contraction properties than $\mathcal{R}$.

Proposition 3.2 *Let s^* be the solution of a Stefan problem with the Neumann condition (or more generally one which satisfies the reversal property of Lemma 3.1). If $s \leq s^*$*

for all t, then

$$s - s^* \leq \frac{s - s^*}{2} \leq \mathcal{P}^{1/2}(s) - s^* \leq \frac{\mathcal{R}(s) - s^*}{2} \leq \mathcal{R}(s) - s^*.$$

If $s \geq s^*$ *for all t*

$$s - s^* \geq \frac{s - s^*}{2} \geq s^* - \mathcal{P}^{1/2}(s) \geq \frac{\mathcal{R}(s) - s^*}{2} \geq \mathcal{R}(s) - s^*.$$

Proof If $s \leq s^*$

$$\mathcal{P}^{1/2}(s) - s^* = \frac{1}{2}(\mathcal{R}(s) + s) - \frac{1}{2}(\mathcal{R}(s^*) + s^*) = \frac{1}{2}(\mathcal{R}(s) - s^*) + \frac{1}{2}(s - s^*) \leq \frac{1}{2}(\mathcal{R}(s) - s^*)$$

and

$$\mathcal{P}^{1/2}(s) - s^* = \frac{1}{2}(\mathcal{R}(s) + s) - s^* = \frac{1}{2}(\mathcal{R}(s^*) - s^*) + \frac{1}{2}(s - s^*) \geq \frac{1}{2}(s - s^*)$$

A similar proof applies when $s > s^*$. □

This result is strengthened in the next proposition, using the Chebyshev norm

$$\|s_1 - s_2\| \equiv \max_{t \in [0,T]} |s_1(t) - s_2(t)|.$$

Proposition 3.3 *Assume* $s_1 \leq s_2$ *or* $s_2 \leq s_1$ *and* $\mathcal{R}$ *satisfies the reversal property of Lemma 3.1. If* $\mathcal{R}$ *is bounded, i.e.,* $\|\mathcal{R}(s_1) - \mathcal{R}(s_2)\| \leq \gamma \|s_1 - s_2\|$ *for finite* γ*, then the following inequalities hold true:*

$$\begin{aligned} |\mathcal{P}^{\alpha}(s_1)(t) - \mathcal{P}^{\alpha}(s_2)(t)| &\leq \max\big(\alpha\gamma,\ 1-\alpha\big)\, \|s_1 - s_2\| \\ \left\|\mathcal{P}^{\frac{1}{\gamma+1}}(s_1) - \mathcal{P}^{\frac{1}{\gamma+1}}(s_2)\right\| &\leq \frac{\gamma}{\gamma+1}\, \|s_1 - s_2\| \leq \|s_1 - s_2\|. \end{aligned} \tag{8}$$

Proof Let $s_1 \leq s_2$ all t, the same proof being valid for the reverse inequality. Then

$$\begin{aligned} (1-\alpha)(s_1 - s_2) \leq \mathcal{P}^{\alpha}(s_1) - \mathcal{P}^{\alpha}(s_2) &= \alpha(\mathcal{R}(s_1) - \mathcal{R}(s_2)) + (1-\alpha)(s_1 - s_2) \\ &\leq \alpha(\mathcal{R}(s_1) - \mathcal{R}(s_2)), \end{aligned}$$

since $s_1 \leq s_2,\ \mathcal{R}(s_1) \geq \mathcal{R}(s_2)$. Now if at some t $\mathcal{P}^{\alpha}(s_1)(t) - \mathcal{P}^{\alpha}(s_2)(t) \geq 0$ then

$$\begin{aligned} |\mathcal{P}^{\alpha}(s_1)(t) - \mathcal{P}^{\alpha}(s_2)(t)| \leq\ & \alpha |\mathcal{R}(s_1)(t) - \mathcal{R}(s_2)(t)| \leq \alpha \max_t |\mathcal{R}(s_1)(t) - \mathcal{R}(s_2)(t)| \\ &= \alpha \|\mathcal{R}(s_1) - \mathcal{R}(s_2)\| \leq \alpha\gamma \|s_1 - s_2\|. \end{aligned}$$

Otherwise if at some t, $\mathcal{P}^\alpha(s_1)(t) - \mathcal{P}^\alpha(s_2)(t) \le 0$ then

$$|\mathcal{P}^\alpha(s_1)(t) - \mathcal{P}^\alpha(s_2)(t)| \le (1-\alpha)|s_1(t) - s_2(t)| \le (1-\alpha)\max_t |s_1(t) - s_2(t)| = (1-\alpha)\|s_1 - s_2\|.$$

Hence,

$$|\mathcal{P}^\alpha(s_1)(t) - \mathcal{P}^\alpha(s_2)(t)| \le \max(\alpha\gamma\|s_1 - s_2\|, (1-\alpha)\|s_1 - s_2\|).$$

Since the above relation is true for all t, we have

$$\max_t |\mathcal{P}^\alpha(s_1)(t) - \mathcal{P}^\alpha(s_2)(t)| \equiv \|\mathcal{P}^\alpha(s_1) - \mathcal{P}^\alpha(s_2)\| \le \max(\alpha\gamma, 1-\alpha)\|s_1 - s_2\|.$$

The best bound is given by $\min_\alpha \max(\alpha\gamma, 1-\alpha)$ which occurs when the two terms $\alpha\gamma, 1-\alpha$ are equal and hence $\alpha = \frac{1}{\gamma+1}$. Thus, we obtain (8). □

We use the above result to establish that for the Neumann problem the fixed point iteration $s_{n+1} = \mathcal{P}^\alpha(s_n)$ converges geometrically when properly initialized.

Proposition 3.4 *For the Neumann problem, consider a boundary $s_1 \ge s^*$ and let $\mathcal{R}$ be bounded by γ. Then the fixed point iteration $s_{n+1} = \mathcal{P}^\alpha(s_n)$ initialized with either $s_1 \ge s^*$ or $s_0 \le s^*$ converges geometrically to s^* for $\alpha \le \frac{1}{\gamma+1}$.*

Proof A boundary $s_1 \ge s^*$ can be easily obtained for a Neumann problem as shown earlier, and similarly for an $s_0 \le s^*$ since $s_0 = \mathcal{R}(s_1) \le s^*$.

Starting the iteration with s_1, we have $\mathcal{R}(s_1) \le s^* \le s_1$ and $\|\mathcal{R}(s_1) - \mathcal{R}(s^*)\| \le \gamma\|s_1 - s^*\|$ and hence $s^* - \mathcal{R}(s_1) \le \gamma(s_1 - s^*)$ which leads to

$$s^* \le \frac{1}{1+\gamma}\mathcal{R}(s_1) + \frac{\gamma}{1+\gamma}s_1 \le \alpha\mathcal{R}(s_1) + (1-\alpha)s_1 \le s_1.$$

The second and third inequalities above are valid for $\alpha \le \frac{1}{1+\gamma}$ since $\mathcal{R}(s_1) \le s^* \le s_1$ and therefore the sequence $s_{n+1} = \mathcal{P}^\alpha(s_n)$ is decreasing and bounded below by the fixed point s^*. Note that

$$\|s_{n+1} - s^*\| = \|\mathcal{P}^\alpha(s_n) - \mathcal{P}^\alpha(s^*)\| \le \max(\alpha\gamma, 1-\alpha)\|s_n - s^*\|.$$

The coefficient $\max(\alpha\gamma, 1-\alpha) = \beta$ is less than 1 for $\alpha \le \frac{1}{\gamma+1}$ and thus convergence is geometric since $\|s_{n+1} - s^*\| \le \beta\|s_n - s^*\|$.

Starting the iteration with $s_0 \le s^*$, we have $\mathcal{R}(s_0) \ge s^*$, $\|\mathcal{R}(s_0) - \mathcal{R}(s^*)\| \le \gamma\|s_0 - s^*\|$ and hence $\mathcal{R}(s_0) - s^* \le \gamma(s^* - s_0)$ which leads to

$$s^* \ge \frac{1}{1+\gamma}\mathcal{R}(s_0) + \frac{\gamma}{1+\gamma}s_0 \ge \alpha\mathcal{R}(s_0) + (1-\alpha)s_0 \ge s_0.$$

The second and third inequalities above are valid for $\alpha \leq \frac{1}{1+\gamma}$ since $\mathcal{R}(s_0) \geq s^* \geq s_0$ and therefore the sequence $s_{n+1} = \mathcal{P}^\alpha(s_n)$ is increasing and bounded above by the fixed point s^*. Again

$$\|s_{n+1} - s^*\| = \|\mathcal{P}^\alpha(s_n) - \mathcal{P}^\alpha(s^*)\| \leq \max(\alpha\gamma, 1-\alpha)\|s_n - s^*\|.$$

and geometric convergence follows for $\alpha \leq \frac{1}{\gamma+1}$. □

The fastest convergence is achieved when α is as large as possible, i.e $\frac{1}{\gamma+1}$ in which case the convergence rate is $\frac{\gamma}{1+\gamma}$. In case γ is not known a priori, the algorithm can be implemented by starting with a reasonable α and halving it in case it does not generate decreasing (increasing) boundaries. Our implementation started with an $\alpha = \frac{1}{2}$ and converged in all cases examined.

Applying the algorithm to Dirichlet problems gave unexpectedly good results, and thus we will state it for both problems. For Dirichlet problems there is no lower bound for the boundary, and hence we have to start with a low initial boundary. Since it is not known how small a boundary is required, the algorithm will restart using a lower initial boundary in case it failed to converge. A description of the algorithm follows, while implementation details are provided in Sect. 6.

Description of the $\mathcal{P}^\alpha$ algorithm for the Stefan problem.

1. Set iteration counter n to zero.
   Set $\alpha = \alpha_0$.
   Select an initial boundary $s_0 \geq s^*$ if available and set Case $\leftarrow$ High.
   If such an s_0 is not available select $s_0 \approx 0$ and set Case $\leftarrow$ Low.
2. Solve the Fixed Boundary Neumann problem.
   i.e., the heat equation (2) with $U(s_n(t), t) = 0$, $U_x(0, t) = -h(t)$.
   OR Solve the Fixed Boundary Dirichlet problem
   i.e., the heat equation (2) with $U(s_n(t), t) = 0$, $U(0, t) = g(t)$.
3. Given the solution U of Step 1 evaluate $\mathcal{R}$, $\mathcal{P}^\alpha(s_n)$
4. With Case=High, IF $\mathcal{P}^\alpha(s_n)$ is not below s_n decrease α by say halving it and **restart** the algorithm ELSE Update the boundary by $s_{n+1} \leftarrow \mathcal{P}^\alpha(s_n)$
5. With Case=Low, If $\mathcal{P}^\alpha(s_n)$ is not above s_n decrease α by say halving it and **restart** the algorithm ELSE Update the boundary by $s_{n+1} \leftarrow \mathcal{P}^\alpha(s_n)$
6. $n \leftarrow n + 1$
7. If $s_n \approx s_{n-1}$, the algorithm terminates.
   ELSE: IF the iteration limit has not been reached GO TO Step 1 using the new boundary s_n.
   ELSE: (The iteration limit has been reached without convergence) Reduce s_0, $n \leftarrow 0$ and GO TO Step 1.

3.2 Reversal in the fixed boundary Dirichlet problem

We subsequently demonstrate that, even in the Dirichlet problem, $\mathcal{R}$ possesses the reversal property and thus an $\mathcal{R}$ iteration would converge subject to the caveats stated in the beginning of this section.

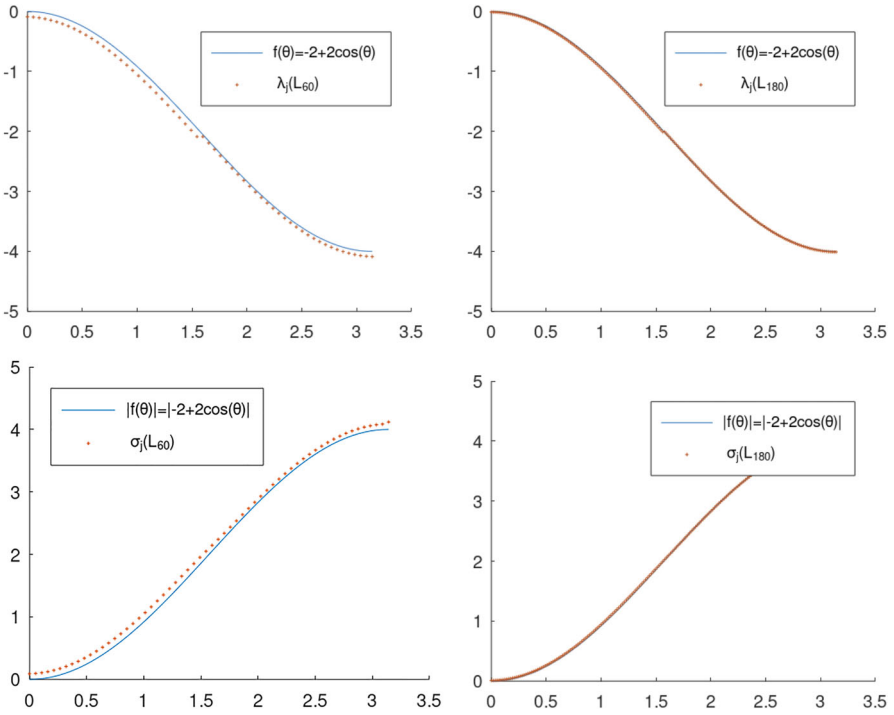


Fig. 2 The top-left and top-right panels display the eigenvalues alongside the graph of the GLT symbol. The bottom-left and bottom-right panels show the singular values together with the absolute value of the GLT symbol

Lemma 3.5 *Consider the Fixed Boundary Dirichlet Problem with $U^s(0,t) = g(t)$, g nonnegative and nondecreasing. Then for a given boundary s the solution U^s satisfies $U^s_x(0,t) \leq 0$.*

Proof Consider the problem in $Q_{s,T}$ i.e., $t \in [0,T]$. The maximum of U^s is on the parabolic boundary and since $U^s(s(t),t) = 0$ the maximum is at $x = 0,\ t = T$ where $U^s(0,T) = g(T)$ given that g is nondecreasing. Hence $U^s_x(0,T) \leq 0$ for otherwise the maximum would not be on the parabolic boundary. Since g is nondecreasing, the argument can be repeated for any value of T. □

Although we will not directly use the above lemma, it remains interesting in its own right. Notably, it does not hold for functions g's that exhibit both increasing and decreasing regions, as can be verified (see Fig. 6 in Sect. 6) through direct calculation.

Lemma 3.6 *For Fixed Boundary Dirichlet problems with boundaries $s_1 \leq s_2$ and for which $U^{s_1}(0,t) = U^{s_2}(0,t) = g(t)$, we have $U^{s_1}_x(0,t) \leq U^{s_2}_x(0,t)$.*

Proof Consider $\Delta U(t) = U^{s_2}(x,t) - U^{s_1}(x,t)$ in $Q_{s_1,T}$. $\Delta(x,t)$ vanishes for $x = 0$ and is nonnegative on s_1. The minimum of ΔU is on the parabolic boundary and in particular for some zero x and some t. But then $\Delta U_x(0,t)$ must be

nonnegative, otherwise there is a minimum in the parabolic interior. Therefore, $\Delta U_x(0,t) = U_x^{s_2}(0,t) - U_x^{s_1}(0,t) \geq 0$ as required. □

The main result for Dirichlet problems is the following:

Proposition 3.7 *The operator $\mathcal{R}$ as defined in (6) for the Fixed Boundary Dirichlet problem with nonnegative boundary condition $U(0,t) = g(t) \geq 0$ has the reversal property of Lemma 3.1, i.e., if s_1, s_2 are boundary functions and $s_1(t) \leq s_2(t),\ t \in [0,T]$, then $\mathcal{R}(s_1)(t) \geq \mathcal{R}(s_2)(t)$.*

Proof Consider the boundary functions (smooth and starting at the origin) s_1, s_2 and such that $s_1(t) \leq s_2(t),\ t \in [0,T]$ and the corresponding solutions $U^{s_1}(x,t), U^{s_2}(x,t)$ for $x \leq s_1(t)$. On s_1 we have $U^{s_2}(s_1(t),t) - U^{s_1}(s_1(t),t) \geq 0$ and at zero $U^{s_2}(0,t) - U^{s_1}(0,t) = g(t) - g(t) = 0$. Hence, by the minimum principle $U^{s_2}(x,t) - U^{s_1}(x,t) \geq 0$ for $x \leq s_1(t)$. We also have by Lemma 3.6 $U_x^{s_1}(0,t) \leq U_x^{s_2}(0,t)$. Hence, using expression (2.1) for $\mathcal{R}$, we have

$$\mathcal{R}(s_2)(t) - \mathcal{R}(s_1)(t) = -\int_0^t [U_x^{s_2}(0,\tau) - U_x^{s_1}(0,\tau)]\mathrm{d}\tau - \int_0^{s_2(t)} U^{s_2}(x,t)\mathrm{d}x + \int_0^{s_1(t)} U_x^{s_1}(x,t)\mathrm{d}x.$$

The first term is non-positive by the previous lemma. The last two terms are

$$-\int_0^{s_2(t)} U^{s_2}(x,t)\mathrm{d}x + \int_0^{s_1(t)} U^{s_1}(x,t)\mathrm{d}x = \int_0^{s_1(t)} [U^{s_1}(x,t) - U^{s_2}(x,t)]\mathrm{d}x - \int_{s_1(t)}^{s_2(t)} U^{s_2}(x,t)\mathrm{d}x.$$

Both terms in the above expression are non-positive by our previous lemmas, and thus $\mathcal{R}$ has the desired property. □

3.3 Inhomogeneous solid phase

The reversal property is also valid for problems with an inhomogeneous solid phase where the β coefficient depends on position, the Stefan condition is (2) and the proper transform is the non-simplified (6). For ease of notation, we set $\delta(x) = 1/\beta(x)$, and write

$$\mathcal{R}(s)(t) = -\int_0^t \delta(s(z)) U_x^s(s(z),z)\mathrm{d}z.$$

We next derive an alternative expression for $\mathcal{R}$ taking into account the inhomogeneity.

Lemma 3.8

$$\mathcal{R}(s)(t) = -\int_0^{s(t)} \delta(x)U^s(x,t)\mathrm{d}x - \int_0^t \delta(0)U_x^s(0,\tau)\mathrm{d}\tau + \int_0^t \delta'(0)U^s(0,\tau)\mathrm{d}\tau + \int_0^t \int_0^{s(\tau)} \delta''(x)U^s(x,\tau)\mathrm{d}x\mathrm{d}\tau. \tag{9}$$

Proof Consider the integral of the zero expression $(U_t^s(x,t) - U_{xx}^s(x,t))\delta(x)$ on $Q_{s,t} = \{0 < x < s(\tau), \tau \le t\}$, that is

$$0 = \int_0^t \int_0^{s(\tau)} \delta(x)[U_t^s(x,\tau) - U_{xx}^s(x,\tau)]\mathrm{d}x\mathrm{d}\tau.$$

Applying Green's theorem for the vector field $(U^s, 0)$ on the region $Q_{s,T}$, we have

$$\int_0^t \int_0^{s(\tau)} \delta(x)U_t^s(x,\tau)\mathrm{d}x\mathrm{d}\tau = \int_0^{s(t)} \delta(x)U^s(x,t)\mathrm{d}x.$$

For the second term of (10) after two integrations by parts, we obtain:

$$\int_0^t \int_0^{s(\tau)} \delta(x)U_{xx}^s(x,\tau)\mathrm{d}x\mathrm{d}\tau = \int_0^t [\delta(s(\tau))U_x^s(s(\tau),\tau) - \delta(0)U_x^s(0,\tau)]\mathrm{d}\tau + \int_0^t \delta'(0)U^s(0,\tau)\mathrm{d}\tau + \int_0^t \int_0^{s(\tau)} \delta''(x)U^s(x,\tau)\mathrm{d}x\mathrm{d}\tau.$$

Combining the above equations and the definition of $\mathcal{R}$, we obtain the required (9). □

Expression (9) reduces to (2.1) when δ is unity. We next use it to derive some conditions guaranteeing the reversal property.

Proposition 3.9 *Assume that the inhomogeneity function δ is concave. The reversal property holds for the Fixed Boundary Dirichlet problem provided $\delta(0) > 0$ while for the Neumann problem provided $\delta'(0) < 0$.*

Proof If $s_1 \ge s_2$ then $U^{s_1} \ge U^{s_2}$. In the Dirichlet case, the third term in (9) vanishes and the other terms are decreasing in s. In the Neumann case, the term involving $\delta(0)$ is constant and all other terms are decreasing. □

4 The numerical solution of the fixed boundary problems

In this section, we show how to implement Step 2 in the $\mathcal{P}^\alpha$ algorithm in Sect. 3.1, which requires the solution of the Fixed Boundary Problem. We implement the boundary immobilization technique, combined with a Crank–Nicolson scheme, which is

widely used in the numerical treatment of parabolic PDEs. Notably, it has been utilized as a core component of algorithms designed to locate the Stefan interface, as demonstrated in [17, 20]. In this work, we adopt a similar approach, applying the boundary immobilization method with a known boundary s in conjunction with the Crank–Nicolson scheme. This combination facilitates an efficient and accurate computation of the evolving boundary. We then set $\xi = x/s(t)$ $s(t) \neq 0$ and $F(\xi, t) = U(s(t)\xi, t)$ where U is the solution of a Fixed Boundary Dirichlet or Neumann problem. Since $F_\xi(\xi, t) = U_x(s(t)\xi, t)s(t)$, $F_t(\xi, t) = U_t(s(t)\xi, t) + U_x(s(t)\xi, t)s'(t)\xi$, $F_{\xi\xi}(\xi, t) = U_{xx}(s(t)\xi, t)s^2(t)$, the heat equation (2) becomes for $s(t) \neq 0$

$$F_{\xi\xi}(\xi, t)/s^2(t) = F_t(\xi, t) - s'(t)\xi F_\xi(\xi, t)/s(t).$$

The boundary conditions are $F(1, t) = U(s(t), t) = 0$ and $F(0, t) = U(0, t) = g(t)$ in the Dirichlet case, $F_\xi(0, t) = U_x(0, t)s(t) = -h(t)s(t)$ in the Neumann case. The Stefan condition is $\beta(s^*(t))s^*(t)' = -U_x(s^*(t), t) = -F_\xi(1, t)/s^*(t)$, but will not be explicitly used in our method as is done in alternative ones, and will just verify it after convergence.

As stated in the Algorithm description in the previous Section, we update the boundaries through the iteration

$$s_{n+1}(t) = \mathcal{P}^\alpha(s_n)(t) = \alpha\mathcal{R}(s_n)(t) + (1 - \alpha)s_n(t),$$

where the operator $\mathcal{R}$ is in terms of F following the change of variable from x to ξ

$$\mathcal{R}(s)(t) = -\int_0^{s(t)} U_x(x, t)\mathrm{d}x = -\frac{1}{s^2(t)}\int_0^1 F_\xi(\xi, t)\mathrm{d}\xi.$$

Care must be taken when t is close to zero for then the integrand is divided by $s^2(t)$ that tends to zero.

To solve the Fixed Boundary Problems, we discretize (10) by the Crank–Nicolson scheme involving a central difference at time $t^{n-\frac{1}{2}}$ and a second-order central difference for space derivative. Setting $F_i^n = F(i\Delta\xi, n\Delta t)$, $i = 1, 2, \ldots, N-1$, $N = 1/\Delta\xi$, $n = 1, 2, \ldots, T/\Delta t$, $z(t) = s^2(t)$, we are led to the discretization scheme

$$\frac{1}{2}\left(\frac{F_{i+1}^n - 2F_i^n + F_{i-1}^n}{\Delta\xi^2}\right) + \frac{1}{2}\left(\frac{F_{i+1}^{n-1} - 2F_i^{n-1} + F_{i-1}^{n-1}}{\Delta\xi^2}\right) = z^{n-\frac{1}{2}}\left(\frac{F_i^n - F_i^{n-1}}{\Delta t}\right) - \frac{\xi_i}{2}\left(\frac{dz}{dt}\right)^n\left[\frac{1}{2}\left(\frac{F_{i+1}^n - F_{i-1}^n}{2\Delta\xi}\right) + \frac{1}{2}\left(\frac{F_{i+1}^{n-1} - F_{i-1}^{n-1}}{2\Delta\xi}\right)\right]$$

and equivalently to

$$(F_{i+1}^n - 2F_i^n + F_{i-1}^n) + (F_{i+1}^{n-1} - 2F_i^{n-1} + F_{i-1}^{n-1}) = z^{n-\frac{1}{2}}\frac{2\Delta\xi^2}{\Delta t}(F_i^n - F_i^{n-1})$$

$$-\frac{\xi_i}{4}\left(\frac{dz}{dt}\right)^n \Delta\xi\left[(F_{i+1}^n - F_{i-1}^n) + (F_{i+1}^{n-1} - F_{i-1}^{n-1})\right],$$

where $z^n = z(n\Delta t)$, $z^{n-\frac{1}{2}} = \frac{z^n + z^{n-1}}{2}$ and $\left(\frac{dz}{dt}\right)^n = \frac{z^n - z^{n-1}}{\Delta t}$.

Setting $\rho^n = z^{n-\frac{1}{2}}\frac{2\Delta\xi^2}{\Delta t}$ and $\sigma_i^n = \frac{\xi_i}{4}\left(\frac{dz}{dt}\right)^n \Delta\xi$, the above equation becomes

$$\begin{aligned}
&(F_{i+1}^n - 2F_i^n + F_{i-1}^n) + (F_{i+1}^{n-1} - 2F_i^{n-1} + F_{i-1}^{n-1}) = \rho^n(F_i^n - F_i^{n-1})\\
&\quad - \sigma_i^n[(F_{i+1}^n - F_{i-1}^n) + (F_{i+1}^{n-1} - F_{i-1}^{n-1})] \Rightarrow\\
&(1-\sigma_i^n)F_{i-1}^n - (2+\rho^n)F_i^n + (1+\sigma_i^n)F_{i+1}^n\\
&= -(1-\sigma_i^n)F_{i-1}^{n-1} + (2-\rho^n)F_i^{n-1} - (1+\sigma_i^n)F_{i+1}^{n-1}.
\end{aligned} \tag{10}$$

This is valid for $i = 1, \ldots, N-1$, while for $i = 0$, taking into account that $\sigma_i^n = 0$ and replacing the term F_{-1}^n using the relationship $\frac{F_1^n - F_{-1}^n}{2\Delta\xi} = h^n s^n \Rightarrow F_{-1}^n = F_1^n - 2\,h^n s^n \Delta\xi$, with $s^n = s(n\Delta t)$, $h^n = h(n\Delta t)$. Thus, the discretization (10) leads to the equation

$$-(2+\rho^n)F_0^n + 2F_1^n = (2-\rho^n)F_0^{n-1} - 2F_1^{n-1} + 4\Delta\xi\,\frac{s^n h^n + s^{n-1}h^{n-1}}{2}. \tag{11}$$

Since $U(s(t), t) = F_N^n = 0$, for $i = N$, we have

$$F_N^n = F_N^{n-1} = 0, \quad \text{or} \quad -(2+\rho^n)F_N^n = (2-\rho^n)F_N^{n-1} = 0. \tag{12}$$

Let now $R_{N+1}^n, L_{N+1}^n \in \mathbb{R}^{(N+1)\times(N+1)}$, defined as,

$$L_{N+1}^n = \begin{bmatrix}
-(2+\rho^n) & 2 & & & & & \\
1-\sigma_1^n & -(2+\rho^n) & 1+\sigma_1^n & & & & \\
& 1-\sigma_2^n & -(2+\rho^n) & 1+\sigma_2^n & & & \\
& & \ddots & \ddots & \ddots & & \\
& & & \ddots & \ddots & \ddots & \\
& & & & 1-\sigma_{N-1}^n & -(2+\rho^n) & 1+\sigma_{N-1}^n \\
& & & & & 0 & -(2+\rho^n)
\end{bmatrix}, \tag{13}$$

$$R_{N+1}^n = \begin{bmatrix}
(2-\rho^n) & -2 & & & & & \\
-1+\sigma_1^n & (2-\rho^n) & -1-\sigma_1^n & & & & \\
& -1+\sigma_2^n & (2-\rho^n) & -1-\sigma_2^n & & & \\
& & \ddots & \ddots & \ddots & & \\
& & & \ddots & \ddots & \ddots & \\
& & & & -1+\sigma_{N-1}^n & (2-\rho^n) & -1-\sigma_{N-1}^n \\
& & & & & 0 & (2-\rho^n)
\end{bmatrix}, \tag{14}$$

and $E_{N+1}^n \in \mathbb{R}^{N+1}$ defined as $E_{N+1}^n = [4\Delta\xi \frac{s^n h^n + s^{n-1} h^{n-1}}{2}, 0, \ldots, 0]^T$. Given the temperature distribution $f_{N+1}^{n-1} = [F_0^{n-1}, F_1^{n-1}, \ldots, F_N^{n-1}]^T$, the equations (11)-(12) can be written in matrix form

$$L_{N+1}^n f_{N+1}^n = R_{N+1}^n F_{N+1}^{n-1} + E_{N+1}^n, \tag{15}$$

for $N = 1, 2, \ldots$ and $f_{N+1}^0 = [0, 0, \ldots, 0]^T$.

5 Spectral analysis of the coefficient matrix-sequence

In this section, we provide a study on the matrix-sequence $\{L_N^n\}_N$ (13) which formulate the coefficient matrix of the system. We specifically prove that the matrix sequence belongs to the unilevel scalar $*-$algebra of Generalized Locally Toeplitz (GLT) matrix sequences [11] and we identify its spectral symbol. Furthermore, we prove that the matrix sequence has a GLT momentary symbol expansion which we also identify, see [2–4].

5.1 Eigenvalue and singular value distribution of matrix-sequences

An explicit characterization of the eigenvalues or singular values of matrix sequences of interest has been shown to be feasible only in exceptional cases. Nevertheless, when a matrix sequence arises from the discretization of an infinite-dimensional operator, an asymptotic description in terms of a function f as outlined in Definition 5.1, provides a sufficiently precise framework for the development of fast and efficient solvers applicable to a broad class of problems.

Definition 5.1 Let $f : D \subset \mathbb{R}^d \to \mathbb{C}$, $d \geq 1$, be a function such that the Lebesque measure of D, denoted by $\mu(D)$, is finite and non-zero. Then the matrix sequence $\{A_n\}_n$ has an eigenvalue distribution described by f, if

$$\lim_{n\to\infty} \frac{1}{n} \sum_{j=1}^{n} F(\lambda_j(A_n)) = \frac{1}{\mu(D)} \int_D F(f(x))\mathrm{d}x, \quad \forall F \in C_c(\mathbb{C}),$$

where $C_c(\mathbb{C})$ is the set of all continuous functions with bounded support defined on $\mathbb{C}$. The function f is referred to as the eigenvalue or spectral symbol of the matrix sequence $\{A_n\}_n$ and we write $\{A_n\}_n \sim_\lambda f$.

The matrix sequence $\{A_n\}_n$ has a singular value distribution described by f, if

$$\lim_{n\to\infty} \frac{1}{n} \sum_{j=1}^{n} F(\sigma_j(A_n)) = \frac{1}{\mu(D)} \int_D F(|f(x)|)\mathrm{d}x, \quad \forall F \in C_c(\mathbb{R}),$$

where $C_c(\mathbb{R})$ is the set of all continuous with bounded support functions defined on $\mathbb{R}$. In this case, the function f is referred to as the singular value symbol of the matrix

sequence $\{A_n\}_n$ and we write $\{A_n\}_n \sim_\sigma f$.
If f is both the eigenvalue and singular value symbol of $\{A_n\}_n$ we may write $\{A_n\}_n \sim_{\lambda,\sigma} f$.

Remark 5.1 The meaning of the above definition is that if $d \geq 1$ and the matrix-sequence $\{A_n\}_n$ has an eigenvalue (singular value) distribution described by $f : D \subset \mathbb{R}^d \to \mathbb{C}$, then under the condition that f is continuous almost everywhere (a.e.) a proper rearrangement of the eigenvalues (singular values) of A_n is close to a sampling of f ($|F|$) over an equispaced grid on D, for n large enough. This definition allows eigenvalues (singular values) to be out of the range of f; however, the total number of such eigenvalues (singular values) is at most $o(n)$.

5.2 GLT matrix sequences

We refer the reader to [11] and [12] for a comprehensive exposition of the Generalized Locally Toeplitz (GLT) class, its underlying framework, and its wide range of applications. Here, we limit our discussion to the essential properties required for the characterization and analysis of the matrix sequences of interest.

In summary, the GLT class is constructed from three principal (and simplest, in the sense that each has a distinct and specific definition) building blocks, namely

- Toeplitz matrix sequences generated by a function in $L^1([-\pi,\pi])$. The involved matrices are constant along diagonals. In our setting, each Toeplitz matrix sequence is associated with a Lebesgue integrable function $f(\theta) \sim \sum_{k=-\infty}^{\infty} a_k e^{\mathbf{i}k\theta}$ over $[-\pi,\pi]$, the right part of the equality being the Fourier series of the function, defined on $[-\pi,\pi]$ and periodically extended on the whole real line. The Fourier coefficients a_k of f that is

$$a_k = \frac{1}{2\pi}\int_{[-\pi,\pi]} f(\theta)e^{-\hat{\imath}\,k\theta}\,d\theta \in \mathbb{C}, \quad k \in \mathbb{Z},\ \hat{\imath}^2 = -1,$$

for $k = -n+1,\ldots,n-1$, are arranged on the diagonals of the matrix of order n as follows:

$$T_n(f) = \begin{bmatrix} a_0 & a_{-1} & \cdots & a_{-n+2} & a_{-n+1} \\ a_1 & a_0 & a_{-1} & & a_{-n+2} \\ \vdots & a_1 & a_0 & \ddots & \vdots \\ a_{n-2} & & \ddots & \ddots & a_{-1} \\ a_{n-1} & a_{n-2} & \cdots & a_1 & a_0 \end{bmatrix}.$$

The k-th Fourier coefficient appears on the diagonal where the difference row–column index equals k. The function f is called the *generating function* of $T_n(f)$ and of the whole matrix sequence $\{T_n(f)\}_n$.
Spectral properties of Toeplitz matrices have been widely studied, starting from [14] where Szegő first proved that the eigenvalues of the Toeplitz matrix sequence

$\{T_n(f)\}_n$ generated by a real-valued function $f \in L^\infty([-\pi, \pi])$ are asymptotically distributed as f in the sense of the first part of Definition 5.1. In [26, 27], the same result extended to real or complex-valued functions $f \in L^1([-\pi, \pi])$. For a rich analysis also from a operator point of view, see [15, 28] and references therein.

Theorem 5.2 *Let $f \in L^1([-\pi, \pi])$ and $\{T_n(f)\}_n$ be the Toeplitz matrix-sequence generated by f. Then*

$$\{T_n(f)\}_n \sim_\sigma f.$$

If f is real-valued a.e., then the generated matrices are Hermitian and

$$\{T_n(f)\}_n \sim_\lambda f.$$

- Diagonal sampling matrix sequences generated by a Riemann integrable function α defined on a domain D. These are diagonal matrices whose diagonal elements are a sampling of α on an equispaced grid on D. Of course, for a matrix sequence $\{A_n\}_n$ whose diagonal elements are samplings of a function α, we have $\{A_n\}_n \sim_{\lambda,\sigma} \alpha$. We here are interested in such matrices where α is a continuous function a.e. on $[0,\ 1]$, i.e., α is Riemann integrable over $[0, 1]$. Hence, we define $D_n(\alpha)$ as

$$D_n(\alpha) = \text{diag}_{i=1,\ldots,n}\alpha\left(\frac{i}{n}\right) = \begin{bmatrix} \alpha(\frac{1}{n}) & & & \\ & \alpha(\frac{2}{n}) & & \\ & & \ddots & \\ & & & \alpha(1) \end{bmatrix}.$$

- Zero-distributed matrix-sequences. In accordance with Definition 5.1, these are matrix sequences $\{Z_n\}_n$ such that $\{Z_n\}_n \sim_\sigma 0$. That is,

$$\lim_{n\to\infty} \frac{1}{n} \sum_{j=1}^{n} F(\sigma_j(Z_n)) = F(0), \quad \forall\, F \in C_c(\mathbb{R}).$$

Consequently, any result obtained through standard algebraic operations, including (pseudo-)inversion under mild assumptions, between GLT matrix sequences remains within the GLT class. For the purposes of this work, the following properties are sufficient to identify and characterize the GLT matrix sequences of interest.

GLT1 Every GLT matrix sequence is related to a unique function $\kappa : [0,\ 1] \times [-\pi,\ \pi] \to \mathbb{C}$, which is the GLT symbol of the matrix-sequence. The singular values of the matrix sequence are distributed as the function κ. If the matrices of the sequence are Hermitian, then the eigenvalues of the matrix sequence are distributed as the function κ. We denote the GLT matrix sequence $\{A_n\}_n$ with GLT symbol κ as

$$\{A_n\}_n \sim_{\text{GLT}} \kappa.$$

GLT2 Every Toeplitz matrix sequence, with generating function $f \in L^1([-\pi, \pi])$ is a GLT matrix sequence, with symbol $\kappa(x, \theta) = f(\theta)$.

GLT3 Every diagonal matrix sequence, whose elements are a uniform sampling of a continuous function a.e. $\alpha : [0,\ 1] \to \mathbb{C}$ is a GLT matrix sequence with symbol $\kappa(x, \theta) = \alpha(x)$.

GLT4 Every zero-distributed matrix sequence is a GLT matrix sequence with symbol $\kappa(x, \theta) = 0$.

GLT5 The set of all GLT matrix sequences is a maximal $*$-algebra. In other words, the GLT class is maximal and it is closed under linear combinations, multiplications, conjugate transpositions, and (pseudo)-inversions, provided that the symbol of the matrix sequence which is (pseudo)-inverted is zero at a set of zero Lebesgue measure. Therefore, a matrix sequence obtained by operations among GLT matrix sequences is GLT with a symbol produced by identical operations among the symbols.

5.3 Toeplitz and GLT momentary symbols

We here provide the basic definitions for the Toeplitz and GLT momentary symbols as updated in [2] while we refer the reader to [3] and [4] for extended analysis of the concept.

Definition 5.2 (Toeplitz momentary symbols) Let $\{X_n\}_n$ be a matrix sequence and assume that there exist matrix sequences $\{A_n^{(j)}\}_n$, $\{R_n\}_n$, scalar sequences $c_n^{(j)}$, $j = 0, \ldots, t$, and Lebesgue integrable functions f_j defined over $[-\pi, \pi]$, t nonnegative integer independent of n, such that

$$\left\{ \frac{R_n}{c_n^{(t)}} \right\}_n \sim_{\text{GLT}} 0,$$

is zero-distributed (as in item **GLT4**),

$$\begin{aligned} &\left\{ \frac{A_n^{(j)}}{c_n^{(j)}} \right\}_n = T_n(f_j), \\ &c_n^{(0)} = 1, \quad c_n^{(s)} = o(c_n^{(r)}), \quad t \geq s > r, \\ &\{X_n\}_n = \{A_n^{(0)}\}_n + \sum_{j=1}^{t} \{A_n^{(j)}\}_n + \{R_n\}_n, \end{aligned}$$

$\{A_n^{(j)}\}_n$, $j = 0, \ldots, t$, not zero-distributed which imply f_j, $j = 0, \ldots, t$, not identically zero almost everywhere. Then, by a slight abuse of notation, the function

$$f_n = f_0 + \sum_{j=1}^{t} c_n^{(j)} f_j,$$

is defined as the Toeplitz momentary symbol for X_n and $\{f_n\}$ is the sequence of Toeplitz momentary symbols for the matrix sequence $\{X_n\}_n$.

Definition 5.3 (GLT momentary symbols) Let $\{X_n\}_n$ be a matrix sequence and assume that there exist matrix-sequences $\{A_n^{(j)}\}_n$, $\{R_n\}_n$, scalar sequences $c_n^{(j)}$, $j = 0, \ldots, t$, and measurable functions f_j defined over $[0, 1] \times [-\pi, \pi]$, t nonnegative integer independent of n, such that

$$\left\{ \frac{R_n}{c_n^{(t)}} \right\}_n \sim_{\text{GLT}} 0,$$

is zero-distributed (as in item **GLT4**),

$$\begin{gathered} \left\{ \frac{A_n^{(j)}}{c_n^{(j)}} \right\}_n \sim_{\text{GLT}} f_j, \\ c_n^{(0)} = 1, \quad c_n^{(s)} = o(c_n^{(r)}), \quad t \geq s > r, \\ \{X_n\}_n = \{A_n^{(0)}\}_n + \textstyle\sum_{j=1}^{t} \{A_n^{(j)}\}_n + \{R_n\}_n, \end{gathered}$$

$\{A_n^{(j)}\}_n$, $j = 0, \ldots, t$, not zero-distributed which imply f_j, $j = 0, \ldots, t$, all not identically zero almost everywhere. Then, with a slight abuse of notation, the function

$$f_n = f_0 + \sum_{j=1}^{t} c_n^{(j)} f_j,$$

is defined as the GLT momentary symbol for X_n and $\{f_n\}$ is the sequence of GLT momentary symbols for the matrix sequence $\{X_n\}_n$.

5.4 GLT characterization and GLT momentary symbol of the matrix sequence $\{L_N^n\}_N$

For the remainder of this section and for simplifying the notation, we omit n since it represent the time dependency and does not affect the matrices as N—the spatial discretization order—tends to infinity.
Having defined $z(t) = s^2(t)$, $\rho = z\frac{2(\Delta\xi)^2}{\Delta t}$ and $\sigma_i = \frac{\xi_i}{4}\frac{dz}{dt}\Delta\xi$ with $\sigma_0 = 0$, we have

$$L_{N+1} = \begin{bmatrix} -(2+\rho) & 2 & & & \\ 1-\sigma_1 & -(2+\rho) & 1+\sigma_1 & & \\ & \ddots & \ddots & \ddots & \\ & & 1-\sigma_{N-1} & -(2+\rho) & 1+\sigma_{N-1} \\ & & & 0 & -(2+\rho) \end{bmatrix}$$

$$= \underbrace{\begin{bmatrix} -2 & 1 & & & \\ 1 & -2 & 1 & & \\ & \ddots & \ddots & \ddots & \\ & & 1 & -2 & 1 \\ & & & 1 & -2 \end{bmatrix}}_{T_{N+1}(f_0(\theta))} + \underbrace{\begin{bmatrix} -\rho & \sigma_0 & & & \\ -\sigma_1 & -\rho & \sigma_1 & & \\ & \ddots & \ddots & \ddots & \\ & & -\sigma_{N-1} & -\rho & \sigma_{N-1} \\ & & & -\sigma_N & -\rho \end{bmatrix}}_{M_{N+1}}$$

$$+ \underbrace{\begin{bmatrix} 0 & 1 & & & \\ 0 & 0 & 0 & & \\ & \ddots & \ddots & \ddots & \\ & & 0 & 0 & 0 \\ & & & -1+\sigma_N & 0 \end{bmatrix}}_{R_{N+1}},$$

with $f_0(\theta) = -2 + 2\cos(\theta)$ and $T_{N+1}(f_0(\theta))$ the Toeplitz matrix generated by f_0. According to the property **GLT2**, the matrix sequence $\{T_N(f_0)\}_N$ is GLT with symbol $\kappa(x,\theta) = f_0(\theta)$. Since z and $\frac{dz}{dt}$ are continuous and bounded $\rho = O((\Delta\xi)^2)$, $\sigma_i = O(\Delta\xi)$ the matrix sequence $\{M_N\}_N$ is zero distributed in the sense of Definition 5.1 and thus according to **GLT4** is also GLT with symbol $\kappa(x,\theta) = 0$. The matrix sequence $\{\frac{R_N}{(\Delta\xi)^s}\}_N$ is also zero-distributed for every positive s since it is of rank 2 for every positive s, and thus GLT with symbol $\kappa(x,\theta) = 0$. Combining the above, according to the property **GLT5**, we take

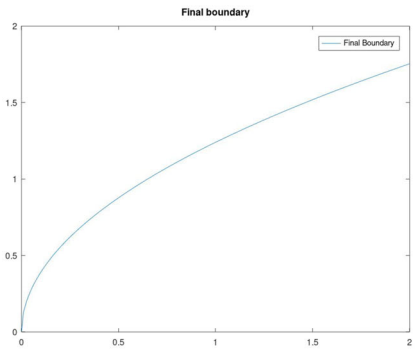
$$\{L_N\}_N \sim_{\text{GLT}} f_0,$$

which according to **GLT1** implies

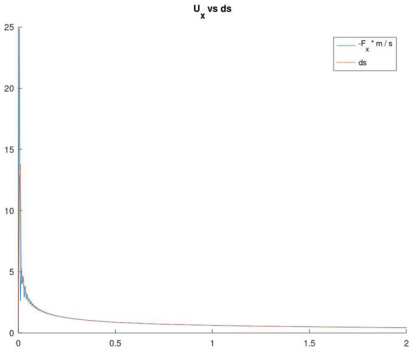
$$\{L_N\}_N \sim_\sigma f_0.$$

In Fig. 2, we present an example to illustrate the precise relationship between the eigenvalues and singular values of a matrix belonging to a GLT matrix sequence and the corresponding GLT symbol of the sequence. For a small matrix size, such as $N = 60$, the eigenvalues and singular values of L_N approximate the curves of the symbol and the absolute value of the symbol, respectively, though a perfect match is not observed. For a moderate matrix size, such as $N = 180$, the match becomes nearly perfect. As N tends to infinity, it is expected that the difference between the eigenvalues and singular values of L_N and the sampling of the function f_0 on a uniform grid over its domain will become infinitesimal. For this example, we used the parameters specified in **Case 1** of the Numerical Experiments section, at time $t = 0.5$, using $\Delta t = 1/200$. Denoting by $D_{N+1}(\hat{\sigma}(\xi))$ the diagonal matrix whose elements are obtained by sampling of $\hat{\sigma}(\xi)$ at equispaced points of an $N+1$-point grid over [0, 1], and

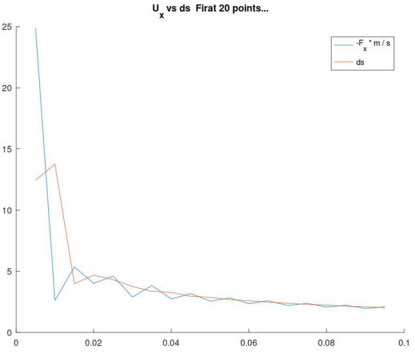
$$\hat{\sigma}(\xi) = \frac{\xi}{4}\frac{dz}{dt},$$



(a) Boundary of Case 1.



(b) Boundary derivative s' vs $-U_x$.



(c) Boundary derivative s' vs $-U_x$ close to the origin.

Fig. 3 Plots of boundary and Stefan conditions of Case 1

$$f_1(\theta) = e^{-\hat{i}\theta} - e^{\hat{i}\theta},$$
$$f_2(\theta) = -\frac{2z}{\Delta t},$$

we receive that

$$\begin{bmatrix} -\rho & \sigma_0 & & & \\ -\sigma_1 & -\rho & \sigma_1 & & \\ & \ddots & \ddots & \ddots & \\ & & -\sigma_{N-1} & -\rho & \sigma_{N-1} \\ & & & -\sigma_N & -\rho \end{bmatrix} = \begin{bmatrix} 0 & \sigma_0 & & & \\ -\sigma_1 & 0 & \sigma_1 & & \\ & \ddots & \ddots & \ddots & \\ & & -\sigma_{N-1} & 0 & \sigma_{N-1} \\ & & & -\sigma_N & 0 \end{bmatrix}$$

$$+\begin{bmatrix} -\rho & & & & \\ & -\rho & & & \\ & & \ddots & & \\ & & & -\rho & \\ & & & & -\rho \end{bmatrix} = \Delta\xi \underbrace{\begin{bmatrix} \hat{\sigma}_0 & & & & \\ & \hat{\sigma}_1 & & & \\ & & \ddots & & \\ & & & \hat{\sigma}_{N-1} & \\ & & & & \hat{\sigma}_N \end{bmatrix}}_{D_{N+1}(\hat{\sigma}(\xi))} \underbrace{\begin{bmatrix} 0 & 1 & & & \\ -1 & 0 & 1 & & \\ & \ddots & \ddots & \ddots & \\ & & -1 & 0 & 1 \\ & & & -1 & 0 \end{bmatrix}}_{T_{N+1}(f_1(\theta))}$$

$$+ (\Delta\xi)^2 \underbrace{\begin{bmatrix} -\hat{\rho} & & & & \\ & -\hat{\rho} & & & \\ & & \ddots & & \\ & & & -\hat{\rho} & \\ & & & & -\hat{\rho} \end{bmatrix}}_{T_{N+1}(f_2(\theta))},$$

We remind the reader that z, $\frac{dz}{dt}$ and Δt are all constants as the infinite discretization is performed in the spatial domain at a specific time t. Applying the properties of the GLT properties, we take

$$D_N(\hat{\sigma}(\xi))T_N(f_1(\theta)) \sim_{\text{GLT}} \hat{\sigma}(\xi) f_1(\theta),$$
$$T_N(f_2(\theta)) \sim_{\text{GLT}} f_2(\theta).$$

Finally, we observe that the conditions of Definition 5.3 are satisfied with:

$$\{L_N\}_N = \{A_0\}_N + \{A_1\}_N + \{A_2\}_N + \{R_N\}_N =$$
$$\{T_N(f_0)\}_N + \Delta\xi\{D_N(\hat{\sigma})T_N(f_1)\}_N + (\Delta\xi)^2\{T_N(f_2)\} + \{R_N\}_N,$$

and $c_N^{(1)} = \Delta\xi$, $c_N^{(2)} = (\Delta\xi)^2$ and $\Delta\xi = \frac{1}{N-1}$. Thus, we conclude that

$$F_N(x,\theta) = f_0(\theta) + \Delta\xi\hat{\sigma}(x) f_1(\theta) + (\Delta\xi)^2 f_2(\theta)$$

is the GLT momentary symbol of L_N and $\{F_N\}$ represents the sequence of GLT momentary symbols for the matrix sequence $\{L_N\}_N$.

6 Numerical experiments

We report on the calculations performed using the $\mathcal{P}^\alpha$ Algorithm described in the end of Sect. 3.1.

Step 2 of the algorithm requires determining U^s for a boundary s in the Fixed Boundary Neumann or Dirichlet Problems and it was carried out by the Crank–Nicolson method outlined in Sect. 4.

Concerning the initial boundary, in view of Proposition 3.4 and the description of the Algorithm, we chose to initialize with the hopefully small boundary $s_0(t) = 0.1 \cdot t$

even in Neumann problems. The last step of the algorithm calls for restarting with an even smaller initial slope in case it fails to converge. However, in all cases, we present next the algorithm did not have to reduce this initial boundary.

We present calculations for several cases, some appearing in the literature, of Neumann and Dirichlet boundary conditions, homogeneous in the Stefan parameter γ or not. The stopping criterion used was $\|s^{n+1} - s_n\| < \epsilon_1$ or $\|s^{n+1} - s_n\|/\|s_n\| < \epsilon_2$ and $\epsilon_1 \approxeq 0.00001$, $\epsilon_2 \approxeq 0.001$. Fewer than 20 iterations were necessary regardless of the initial boundary selection. In each case, we report on the discrepancy between our solution and the exact one whenever it is available. In all cases, we report on the discrepancy of our solution s^* with respect to the Stefan condition i.e., $\|\frac{ds^*}{dt} + \gamma(s^*(t))U_x^{s^*}(s^*(t), t)\|$. In all cases examined, the calculations terminated successfully, and following convergence, the satisfaction of the Stefan condition was guaranteed, which we still verified it numerically.

We consider the following examples appearing in [20]. All are homogeneous, $\delta(x) = 1$.

Case 1 Dirichlet Problem: $U(0, t) = 1$ and hence is not continuous at the origin. The solution is $U(x, t) = 1 - \text{erf}(ax/s)/\text{erf}(a)$, $s(t) = 2a\sqrt{t}$, a satisfying $\sqrt{\pi}a\text{erf}(a)\exp(a^2) = 1$ i.e., $a = 0.6201\ldots$.
Case 2 Dirichlet Problem: $U(0, t) = \exp(t) - 1$.
Case 3 Neumann Problem: $U_x(0, t) = -\exp(t)$.

Cases 2 and 3 have the solution $U(x, t) = \exp(t - x) - 1$ with boundary $s(t) = t$. On the other hand, the following cases do not have analytic solutions, but their numerical solution has been considered in [21] and [23].

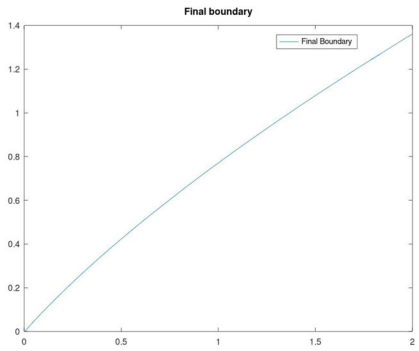
Case 4 Dirichlet Problem [20]: $U(0, t) = 1 - \epsilon \sin(\omega t)$, $\epsilon = 0.5$, $\omega = \pi/2$ discontinuous at the origin.
Case 5 Dirichlet Problem: $U(0, t) = 1 - \exp(-\mu t)$, $\mu = 1$, continuous at the origin.
Case 6 Neumann Problem: $U_x(0, t) = -(1 - \exp(-\mu t))$, $\mu = 1$.
Case 7 Dirichlet Problem: $U(0, t) = t$.
Case 8 Neumann Problem: $U_x(0, t) = -1$.

We also consider Cases 7 and 8 for inhomogeneous ice, with the non homogeneity specified as follows:

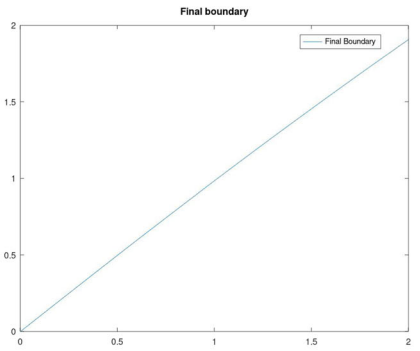
Case 7a Case 7 with $\delta(x) = 1 + x$ which does not satisfy the reversal conditions.
Case 7b Case 7 with $\delta(x) = 2 - x$ which satisfies the reversal conditions.
Case 8a Case 8 with $\delta(x) = 1 + x$ which does not satisfy the reversal conditions.
Case 8b Case 8 with $\delta(x) = 2 - x$ which satisfies the reversal conditions.

We finally consider two inhomogeneous cases with a known exact solution, namely

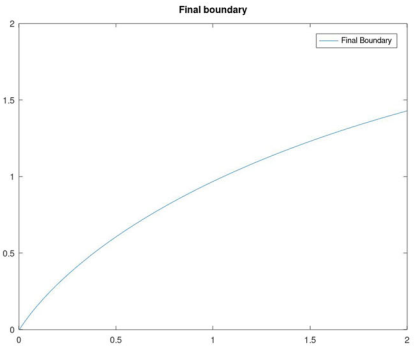
Case 9 Dirichlet BC: $U(0, t) = \exp(t) - 1$ with an inhomogeneity given by $\delta(x) = \frac{x+1}{(x+2)^2}$. The solution is $U(x, t) = \exp(t - x) - (1 + x)$ at the boundary $s(t)$ satisfying $s(t) + \ln(1 + s(t)) = t$. It can be verified by direct calculation that on the above boundary U vanishes and $s'(t) = -\delta(s(t))U_x(s(t), t)$.
Case 10 Neumann BC: $U_x(0, t) = -\exp(t) - 1$ with the same solution and boundary as in Case 9,



(a) Calculated boundary of Case 8.



(b) Calculated boundary of Case 8a.



(c) Calculated boundary of Case 8b.

Fig. 4 The calculated boundaries of 8, 8a, and 8b

The results of our calculations are shown in the following tables. We used a horizon $T = 2$ which is double the one usually found in the literature. We also observed no loss in accuracy even for significantly longer horizons. We considered step sizes $\Delta x = \Delta t = 1/200$ and $1/400$. The convergence criterion was $\|s_{n+1} - s_n\| < \epsilon$ with $\epsilon = 10^{-5}$. The results are in Tables 1 and 2. The discrepancies $\|s^* - s_{exact}\|$ and $\|s^{*\prime} + U_x(s^*, t)\|$ are calculated by the maximum difference either for all t or for t starting from 0.05 to the end of the horizon. The second metric was considerably smaller, showing that there is a high discrepancy near the origin. This behavior persists even for smaller time steps as shown in Table 2 which exhibits only slight improvement in most entries in spite of using half the time step. In the last column of the table, we specify the problem category using the following classification; I: Discontinuous at the origin, II: Continuous at the origin, III: Neumann boundary condition, and IV: Dirichlet boundary condition.

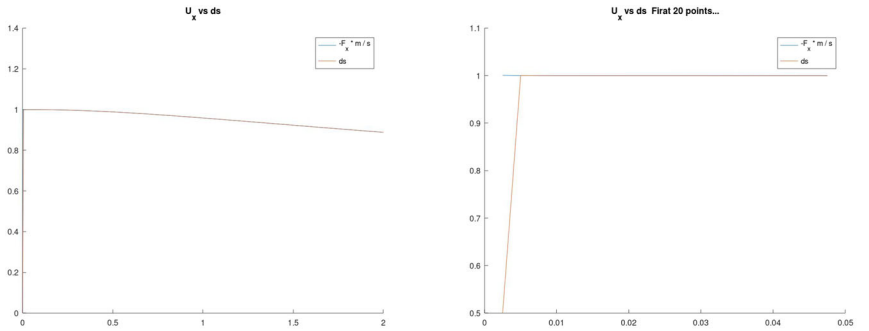
We present some plots related to the calculations. For Case 1, the calculated boundary in Fig. 3a is close to the theoretical one as shown by the small discrepancies in Tables 1 and 2. The Stefan condition comparison of s' and $U_x(s, t)$ is shown in Fig. 3b and near the origin in Fig. 3c where we have higher discrepancy. The results are better

Table 1 Results for $\Delta x = \Delta t = 1/200 \quad T_{horizon} = 2 \quad \epsilon = 10^{-5}$

Case No.	Steps to converge	Discrepancy from exact boundary	Discrepancy from exact boundary 0.05 away	Discrepancy from exact solution	Discrepancy in Stefan condition	Discrepancy in Stefan condition 0.05 away	Category
1	17	0.02545	0.00017	0.00281	12.4480	0.30595	I
2	13	0.00146	0.00007	0.00001	0.7077	0.00029	II
3	11	0.00249	0.00249	0.00110	0.5022	0.00019	III
4	17	–	–	–	12.4390	0.30838	I
5	13	–	–	–	0.7059	0.00181	II
6	13	–	–	–	0.0025	0.00239	III
7	12	–	–	–	0.7068	0.00111	II
8	12	–	–	–	0.4996	0.00199	III
7a	13	–	–	–	0.7081	0.00066	II
7b	11	–	–	–	0.9979	0.00393	II
8a	13	–	–	—	0.5008	0.00018	III
8b	11	–	–	–	0.9942	0.01375	III
9	13	0.00073	0.00023	0.00001	0.3540	0.00030	IV
10	13	0.00142	0.00142	0.00202	0.2506	0.00035	III

Table 2 Results for $\Delta x = \Delta t = 1/400 \quad T_{horizon} = 2 \quad \epsilon = 10^{-5}$

Case No.	Steps to converge	Discrepancy from exact boundary	Discrepancy from exact boundary 0.05 away	Discrepancy from exact solution	Discrepancy in Stefan condition	Discrepancy in Stefan condition 0.05 away	Category
1	18	0.01799	0.00002	0.00281	17.6050	0.15493	I
2	13	0.00073	0.00002	0.00001	0.7074	0.00003	II
3	11	0.00125	0.00120	0.00054	0.5012	0.00018	III
4	17	–	–	–	17.5980	0.15634	I
5	12	–	–	–	0.7065	0.00082	II
6	13	–	–	–	0.0012	0.00119	III
7	12	–	–	–	0.7070	0.00045	II
8	13	–	–	–	0.4999	0.00093	III
7a	13	–	–	–	0.7076	0.00035	II
7b	11	–	–	–	0.9990	0.00176	II
8a	13	–	–	–	0.5004	0.00009	III
8b	11	–	–	–	0.9973	0.00655	III
9	11	0.00037	0.00022	0.00001	0.3538	0.00016	IV
10	13	0.00080	0.00083	0.00011	0.2503	0.00019	III



(a) Boundary derivative s' vs $-U_x$ (b) Boundary derivative s' vs $-U_x$ close to the origin

Fig. 5 Boundary derivative of Case 8a

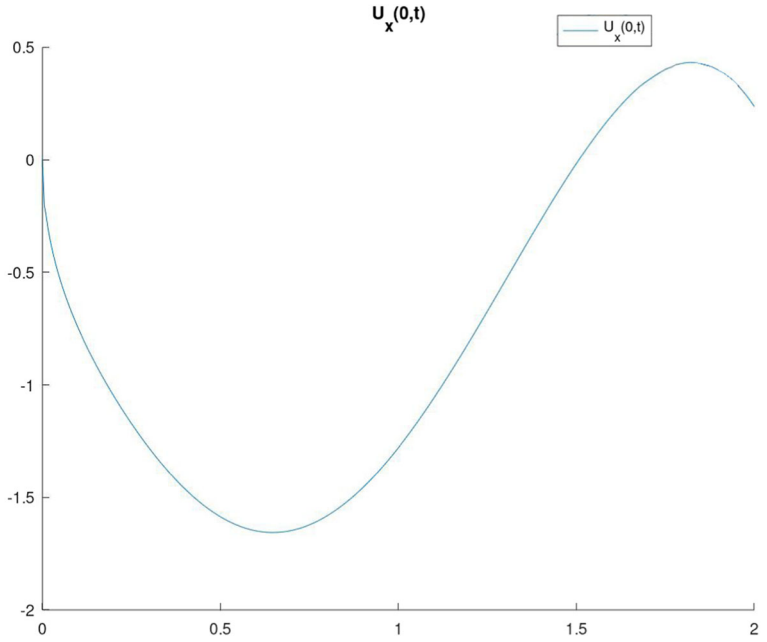


Fig. 6 U_x changes sign on the x axis

for Dirichlet problems with continuous boundary conditions $g(0) = 0$ and in Neumann problems.

It is remarkable that all inhomogeneous problems (7a,b and 8a,b) were successfully solved by the algorithm although 7a,8a do not satisfy the sufficiency conditions in Proposition 3.9. We present the boundary obtained and some Stefan comparisons for cases 8,8a,8b in Figs. 4a–c, 5a, b. Finally, the calculations for the inhomogeneous Cases 9 and 10 are in complete agreement with the exact results, both for the boundary and for the temperature distribution. We include Diagram 7 showing the exact boundary

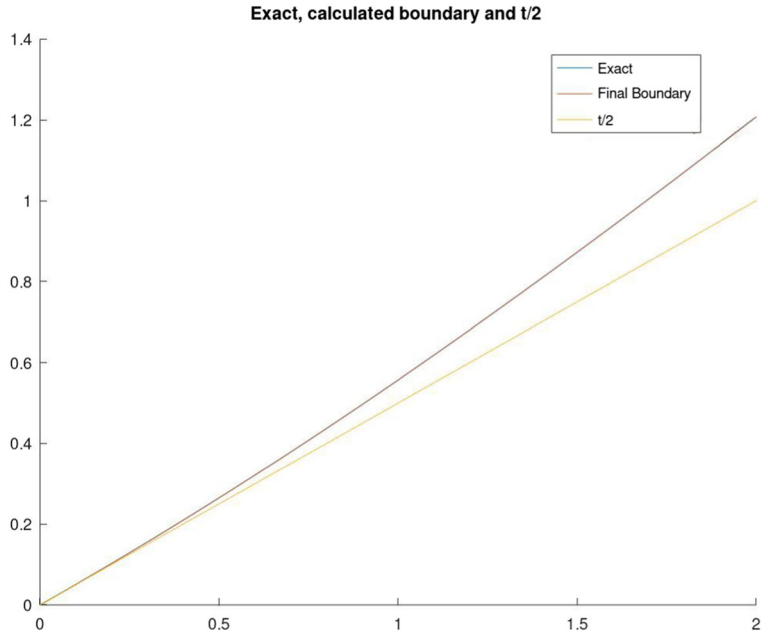


Fig. 7 Case 9: Exact and Calculated Boundary

$s(t) + \ln(1 + s(t)) = t$ that coincides with the calculated one. The diagram includes for illustration purposes the graph of $t/2$ which is tangent to it at the origin.

We also ran a Dirichlet problem with the initial condition $g(0, t) = t^2(t - 2)^2$ with a horizon $T_{hor} = 2$ which has both increasing and decreasing parts; we then computed $U_x(0, t)$ which is shown in Fig. 6. The derivative has both positive and negative values and thus verifies the claim after Lemma 3.5.

7 Conclusions

In this concluding section, we present a short list of open problems and related remarks, which have the potential to lead to further fruitful investigations.

The results in Sect. 6 exhibit consistently rapid convergence, surpassing the guarantees provided by our current theoretical analysis, which applies only to the Neumann case and small values of α. It would be interesting to extend them to explain this fortuitous situation, especially since we used throughout the operator $\mathcal{P}^{1/2}$ which is a contraction only if $\mathcal{R}$ is bounded by $\gamma = 1$. Furthermore, in Neumann problems, the bound of $\mathcal{R}$ increases with the horizon [1], seemingly requiring small values of α for convergence.

We have also considered boundary updates obtained by minimizing Stefan discrepancy functionals such as $\int_0^T (U_x^{s_n}(y(t), t) + \dot{y}(t))^2 dt$ with U^{s_n}, s_n the function and boundary of some iteration n. It can be shown that $y(t) = \mathcal{R}(s(t))$ is an approximate solution to this calculus of variations problem provided s_n is close to the optimal

boundary. Consequently, we tested for faster convergence if we initially use $\mathcal{P}^{1/2}$ until a tolerable Stefan discrepancy is achieved, and then use $\mathcal{P}^{\alpha}$ with α closer to 1 in which case $\mathcal{P}^{\alpha} \approx \mathcal{R}$. Indeed, we observed that convergence was accelerated by about 30% for some choices of the α and boundary proximity parameters. We are studying parameter selections for variable α algorithms that provide consistent acceleration. Such functional minimization updates are interesting since they are similar to the one employed in [18] and which exhibits quadratic convergence. In addition, the boundary transformations used here do not easily generalize while minimization arguments are straightforward to apply for higher dimensions.

Finally, the spectral analysis presented in Sect. 5 is only an initial step toward fast solvers. In fact, given the GLT structure of the involved matrix-sequences, good candidates are the multi-iterative techniques designed in [8, 13, 24], in which multigrid and classical stationary and nonstationary solvers are combined using the spectral information.

Funding Open access funding provided by HEAL-Link Greece.

Data availability The datasets generated and/or analyzed during the current study, as well as the computational codes used to produce the results, are available from the corresponding author on reasonalble request.

Open Access This article is licensed under a Creative Commons Attribution 4.0 International License, which permits use, sharing, adaptation, distribution and reproduction in any medium or format, as long as you give appropriate credit to the original author(s) and the source, provide a link to the Creative Commons licence, and indicate if changes were made. The images or other third party material in this article are included in the article's Creative Commons licence, unless indicated otherwise in a credit line to the material. If material is not included in the article's Creative Commons licence and your intended use is not permitted by statutory regulation or exceeds the permitted use, you will need to obtain permission directly from the copyright holder. To view a copy of this licence, visit http://creativecommons.org/licenses/by/4.0/.

References

1. Andreucci, D.: Lecture notes on the Stefan problem, in: Quaderno del Dottorato "Metodi e Modelli Matematici per la Tecnologia e la Societa ", Dipartimento Metodi e Modelli Matematici, Universita di Roma la Sapienza, (2003)
2. Barakitis, N., Loi, V., Serra-Capizzano, S.: A note on eigenvalues and singular values of variable Toeplitz matrices and matrix-sequences with application to variable two-step BDF approximations to parabolic equations. In *Proceedings of the International Conference on "Spectral and Approximation Theory"*. Springer, 2023. In press
3. Bolten, M., Ekström, S.E., Furci, I., Serra-Capizzano, S.: Toeplitz momentary symbols: definition, results, and limitations in the spectral analysis of structured matrices. Linear Algebra Appl. **651**, 51–82 (2022)
4. Bolten, M., Ekström, S.E., Furci, I., Serra-Capizzano, S.: A note on the spectral analysis of matrix-sequences via glt momentary symbols: from all-at-once solution of parabolic problems to distributed fractional order matrices. Electron. Trans. Numer. Anal. **58**, 136–163 (2023)
5. Cannon, J.R.: The one-dimensional heat equation. Encyclopedia of mathematics and its applications. Cambridge University Press, Cambridge (1984)
6. Cannon, J.R., Denson Hill, C.: Existence, uniqueness, stability, and monotone dependence in a Stefan problem for the heat equation. J. Appl. Math. Mech. **17**(4), 1–20 (1967)
7. Cannon, J.R., Denson Hill, C.: Remarks on a Stefan problem. J. Appl. Math. Mech. **17**(5), 433–441 (1967)

8. Donatelli, M., Garoni, C., Manni, C., Serra-Capizzano, S., Speleers, H.: Robust and optimal multi-iterative techniques for IgA collocation linear systems. Comput. Methods Appl. Mech. Engr. **284**, 1120–1146 (2015)
9. Evans, L.C.: Partial differential equations. American Mathematical Society, 2nd edition, (2010)
10. Friedman, A.: Free boundary problems for parabolic equations I. Melting of solids. J. Math. Mech. **8**(4), 499–517 (1959)
11. Garoni, C., Serra-Capizzano, S.: Generalized locally toeplitz sequences: Theory and applications, vol. I. Springer, Cham (2017)
12. Garoni, C., Serra-Capizzano, S.: Generalized Locally Toeplitz Sequences: Theory and Applications, vol. II. Springer, Cham (2018)
13. Greenbaum, H.: Analysis of a multigrid method as an iterative technique for solving linear systems. SIAM J. Numer. Anal. **21**, 473–485 (1984)
14. Grenander, U., Szegő, G.: Toeplitz forms and their applications, 2nd edn. Chelsea Publishing Co., New York (1984)
15. Grudsky, S., Quiroga-Barranco, R., Vasilevski, N.: Commutative C*-algebras of Toeplitz operators and quantization on the unit disk. J. Funct. Anal. **234**, 1–44 (2006)
16. Gupta, S.C.: The classical Stefan problem. Basic concepts, modeling and analysis. Elsevier, Amsterdam (2000)
17. Landau, H.G.: Heat conduction in a melting solid. Q. Appl. Math. **8**, 81–94 (1950)
18. Magirou, E.F., Vassalos, P., Barakitis, N.: A policy iteration algorithm for the american put option and free boundary control problems. J. Comput. Appl. Math. **373**, 112544 (2020)
19. Meirmanov, A.M.: The Stefan Problem, volume 3. Walter de Gruyter, (1992)
20. Mitchell, S.L., Vynnycky, M.: Finite-difference with increased accuracy and correct initialization for one-dimensional Stefan problems. Appl. Math. Comput. **215**, 1609–1621 (2009)
21. Rizwan-dddin: One-dimensional phase change with periodic boundary conditions. Numer. Heat Trans. **35**(4), 361–272 (1999)
22. Rudin, W.: Functional analysis. McGraw-Hill, Inc., 2nd edition, (1991)
23. Savovic, S., Caldwell, J.: Finite-difference solution of one-dimensional Stefan problem with periodic boundary conditions. Int. J. Heat Mass Trans. **46**, 2911–2916 (2003)
24. Serra, S.: Multi-iterative methods. Comput. Math. Appl. **26**, 65–87 (1993)
25. Tarzia, D.A.: A Bibliography on Moving-Free Boundary Problems for the Heat-Diffusion Equation. The Stefan and Related Problems, MAT-Series A (2000)
26. Tilli, P.: A note on the spectral distribution of Toeplitz matrices. Linear Multilinear Algebra **45**, 147–159 (1998)
27. Tyrtyshnikov, E.E., Zamarashkin, N.L.: Spectra of multilevel Toeplitz matrices: Advanced theory via simple matrix relationships. Linear Algebra Appl. **270**, 15–27 (1998)
28. Vasilevski, N.: Commutative algebras of Toeplitz operators on the Bergman space. Operator Theory: Advances and Applications, volume 185. Birkhäuser Verlag, Basel, (1993)

Publisher's Note Springer Nature remains neutral with regard to jurisdictional claims in published maps and institutional affiliations.